IET Signal Processing

Research Article

IET Journals
The Institution of Engineering and Technology

aiMRS: A feature extraction method from MRS signals based on artificial immune algorithms for classification of brain tumours

ISSN 1751-9675
Received on 8th December 2019
Revised 30th March 2020
Accepted on 22nd April 2020
E-First on 5th June 2020
doi: 10.1049/iet-spr.2019.0576
www.ietdl.org

Emre Dandil[1] ✉

[1]*Department of Computer Engineering, Bilecik Seyh Edebali University, Gulumbe Campus, Bilecik, Turkey*
✉ *E-mail: emre.dandil@bilecik.edu.tr*

Abstract: Precise diagnosis of brain tumour by experienced radiologists involves a complex set of processes including magnetic resonance imaging, magnetic resonance spectroscopy (MRS) data and histopathological evaluations. In this study, a new hybrid feature extraction method, called as aiMRS, based on the negative selection algorithm and clonal selection algorithm of artificial immune systems is developed on MRS data for the detection and classification of brain tumours. In the study, differentiation of benign and malignant brain tumours, classification of normal brain tissue and brain tumour, and detection of metastasis and primary brain tumours are performed with high precision using pattern recognition methods based on the proposed aiMRS method. According to the experimental results performed on a large data set created with the MRS data obtained from INTERPRET database, when the proposed feature extraction method applied, classification of normal brain tissue and brain tumours, benign and malignant brain tumours and metastasis and primary brain tumours is achieved with 100, 98.58 and 98.94% accuracy, respectively. These results show that this proposed system can be used as a secondary tool in physicians' decision-making processes for the classification of brain tumours.

1 Introduction

The American Society of Clinical Oncology (ASCO), which is an International Scientific Organisation, declared that the rate of cancer-related deaths continues to rise around the world [1]. Consequently, it is estimated that the number of people dying from cancer will be ∼11 million by 2030 [2]. According to the predictions from the International Agency for Research on Cancer, 24 million new cases are expected to emerge in 2030 and 29 million new cases are expected to occur in 2040 if cancer rates reveal a similar trend [3]. When these statistics are analysed, it is seen that brain cancer death rates tends to increase. According to the Global Cancer Statistics Report published in 2018, central nervous system tumours, especially the brain tumours, are the 19th most common tumour types in the world and ∼297 thousand people die of this disease and 241 thousand new patients are diagnosed every year. According to same report, central nervous system is the first leading cause of the deaths among the dying caused by cancer. In the developed and developing countries, 4–8 new cancer incidences per 100 thousand people are diagnosed. On the other hand, in under-developed and multi-ethnic countries, this rate doubles. Although children have the greatest incidence of the brain tumours, adults between the ages of 45 and 70 rank second in terms of incidence of the brain tumours [4].

The early diagnosis and treatment of cancers is of vital importance depending on where they locate. The accurate determination of the location, contour and type of the tumours and whether it is diagnosed as a malignant tumour by the physician are extremely important tasks for the clinical and medical follow-up of the tumour. These medical procedures directly affect the success of patient treatment. Nowadays, magnetic resonance imaging (MRI) is widely used to diagnose the presence of tumour and to follow-up the progression. It is also vital to follow-up whether the tumour recurs after treatment [5]. However, some critical procedures such as determination of tumour grades, classification of benign and malignant tumours, distinguishing tumours from non-tumour cases (pseudo tumour, necrosis, cyst, multiple sclerosis (MS) lesion, etc.) are quite difficult to be performed using MRI. Biopsy is still used as the gold standard for detecting such cases where MRI is inadequate. However, biopsy has to be performed with great caution since it is an invasive method and carries the risk of damaging the brain tissues. In addition, it is sometimes not possible to perform biopsy for some regions of the brain where access is restricted. Therefore, innovative non-invasive techniques are needed for such regions especially for the brain region.

Recent studies have shown that magnetic resonance spectroscopy (MRS) imaging, which is a non-invasive technique that provides information about the change of metabolites in the brain, can be used to diagnose brain-related disorders [6–10]. In addition to MRI, important information about the grade, type and metabolism of brain tumours can be obtained by using MRS [11–13]. The studies proposed in the literature show that brain tumours can be distinguished from normal brain tissues and benign tumours can be differentiated from malignant brain tumours using MRS signals [14, 15]. Moreover, the grade of tumour can be determined by the obtained MRS signal [16]. However, analysing MRS signals and extracting meaningful information from these signals are very difficult and require considerable expertise for physicians. Therefore, these processes, which are difficult for physicians, can be realised more accurately and quantitatively by computer-aided analysis methods such as signal processing, pattern recognition and artificial intelligence.

There are various studies in the literature for the computer-aided diagnosis of brain tumours using MRS. The preliminary studies proposed for the diagnosis of brain tumour using MRS signals are generally based on the evaluation of the results obtained by the ratio of peak values of metabolites formed in the MRS frequency spectrum to each other [15, 17–22]. Precisely determining the grade and type of the brain tumour is of vital importance for patients with brain tumours since the treatment planning for the patient can be changed according to the basic characteristics of the tumour. This situation is critical for the patient's average life expectancy. In the literature, there are studies on the detection of grade and type of brain tumours using MRS data suggested both by monitoring changes in metabolites and by more advanced machine learning methods. Castillo *et al.* [23] implemented astrocytoma grading by verifying the changes in myo-inositol metabolite level. Porto *et al.* [24] conducted detection of high-grade and low-grade of astrocytoma's by monitoring the changes in the ratios of metabolites in the MRS spectrum. Server *et al.* [25] carried out grading of glioma-type brain tumours using diffusion MRI and MRS data. Bulik *et al.* [16] investigated the

importance of MR spectroscopy data in glioma grading. The findings showed that monitoring the changes and ratios of metabolites in the spectrum of MRS signals can be used in grading of brain tumours.

Some abnormal conditions in the brain can appear as a tumour on the brain MRI. In particular, oedema occurring after brain surgery looks like a recurrent brain tumour on brain images. In addition, some brain diseases such as abscess (ABC), MS, infarct (vascular occlusion) may also be radiologically diagnosed as tumour on the MRI of the brain. Therefore, differentiating these diseases from tumours without performing an operation to the brain is an extremely important process for the patient's treatment planning and quality of life. Detection of pseudo-brain tumours has been one of the research areas conducted using MRS signals in the diagnosis of brain tumours. In a study conducted on this way, Majos *et al.* [26] provided discrimination of tumour and pseudo-tumoural lesions by monitoring the changes in metabolites using MRS signals.

Primary brain tumours which are tumours that develop and grow in different parts of the brain can affect the surrounding regions of the brain. Metastasis (MET) brain tumours which are tumours that develop and grow in other organs such as lung, liver and kidney can spread to the brain through blood. In other words, they metastasise to the brain. Whether a tumour occurs in the brain or it is a MET brain tumour is very important for the treatment method and planning. Georgiadis *et al.* [14] proposed a pattern recognition system for the discrimination of meningioma (MEN) and metastatic brain tumours using support vector machines (SVMs) method. They used the textural MRI image features and the data of MRS signals. As a result of the study, it was emphasised that the designed system can be helpful in providing clinicians a useful second opinion. Similarly, Tsolaki *et al.* [27] proposed a system for the differentiation of glioblastomas from metastatic brain tumours using 3 T MRS and perfusion data.

Many studies on the use of pattern recognition methods and machine learning techniques in the diagnosis of brain tumours using MRS signals are designed as decision support systems (DSSs) [28, 29]. In addition, more comprehensive studies [30, 31] have also been carried out within the EU-funded INTERPRET project [32]. García-Gómez *et al.* [13] proposed an automatic system for the classification of brain tumours by using the data obtained from multicenter INTERPRET [32] and eTUMOUR [33] projects. In another study, Majos *et al.* [34] conducted the brain tumour classification statistically using the MRS data obtained as short time echo (TE) and long TE. Wang *et al.* [12] presented a study using MRI and MRS data to assist radiologists for differentiating benign and malignant brain tumours. In their study, when the results are evaluated, it is seen that the results obtained by using MRS data increased the success of classification. Luts *et al.* [11] performed the classification of different types of brain tumours by combining ten spectroscopic and four textural features using the SVM method. In the study, they compared the results with linear discriminant analysis (LDA) method to assist clinicians in the diagnosis of brain tumours. Devos *et al.* [35] provided automatic discrimination of brain tumour types using both MRS data and MR images. In the study, differentiation between high-grade gliomas and low-grade gliomas was achieved by LDA and SVM methods. In another study, Nachimuthu and Baladhandapani [36] proposed a pattern recognition system using MR images and MRS data. In the study, tumour and oedema tissues were detected using MR images and MRS data to improve classification accuracy and the extracted features were classified using SVM.

In recent years, MRS-based brain tumour detection systems have been implemented as medical DSSs. In one of the studies using DSS [37], high classification performance was achieved using SVM and LDA methods on MRS data obtained from volunteer participants. Tate *et al.* [30] developed a computer-based DSS for diagnosing and grading brain tumours. In experimental studies on INTERPRET database, the designed DSS software successfully classified brain tumours using LDA. Arizmendi *et al.* [7] proposed a method that combines Gaussian decomposition Bayesian neural networks on MRS signals for automated classification of brain tumours. In another study using DSS, Sáez *et al.* [9] evaluated feasibility and potential value of DSS for brain tumour diagnosis based on MRS to assist novice radiologists. Postma *et al.* [8] investigated relevance of single-voxel MRS and multimodal MRI and MRSI features for brain tumour differentiation. Vicente *et al.* [10] evaluated the accuracy of single-voxel MRS classification of childhood brain tumours on MRS.

In this study, a hybrid feature extraction method called as aiMRS based on artificial immune system (AIS) algorithms such as negative selection algorithm (NSA) and clonal selection algorithm (CSA) and a novel computer-assisted method for the detection and classification of brain tumours using MRS data is proposed to improve results of the previous studies. The contributions of this proposed method for the literature are as follows:

(i) Differentiating of brain tumours and normal brain tissues, classification of benign and malignant brain tumours and distinction between primary and metastatic tumours can be achieved with a developed method with high classification performance.
(ii) The results of previous studies are improved with the proposed method and high performance has been achieved in the detection and classification of brain tumours using MRS data.
(iii) The results are improved in previous studies in which INTERPRET database is used.
(iv) Besides being robust, the developed method can perform extremely fast as it does not require heavy computation time and load.
(v) In experimental studies, a detection/classification process on a standard computer could be completed in ∼2 s using the proposed method.
(vi) Performance evaluations of the proposed method are carried out in detail with a large database (INTERPRET) obtained from different imaging devices and centres.

2 ^{1}H proton magnetic resonance spectroscopy (^{1}H-MRS)

^{1}H-MRS is a method of examining the chemical structure of the brain. The most common atomic nuclei used in MRS are ^{1}H (proton), ^{23}Na (sodium) and ^{31}P (phosphorus). Proton MRS is easier to use than sodium and phosphorus. It provides more precise signal-to-noise sensitivity [38]. MRS can be performed within 10–15 min and added to conventional MRI protocols. Biochemical changes in MRS signals can be used to diagnose tumours, strikes to the head, epilepsy, metabolic disorders, infections and psychological disorders. The disease or disorder in brain is not defined with MRS, but at the final decision stage, MRS spectrum signals have to be interpreted by experienced physicians and verified by MR images of brain. Clinical applications of ^{1}H-MRS in terms of technical and hardware have been increased in recent years. ^{1}H-MRS provides biochemical and metabolic information about brain and its tissue. The information obtained using ^{1}H-MRS is independent and quite different from the information obtained through other MR imaging techniques. The dominant metabolites in brain MRS are N-acetyl aspartate (NAA), choline (Cho), creatine (Cr), myo- Inositol (mI), lactate (Lac), lipids (Lip), glutamine/glutamate (Glx) and amino acids. Besides, the most common ratios of the metabolites used to analyse brain diseases are NAA/Cr, NAA/Cho and Cho/Cr [39]. The peak values and characteristics of the short-TE of ^{1}H-MRS metabolites of the human brain are presented in Table 1.

MRS signals can be acquired as single-voxel and multi-voxel. The results of MRS imaging are observed with resonance spectrum peaks on the *x*-axis as the parts per one million (ppm) units. The ppm scale is read from right to left. Each metabolite appears at a specific peak value. Moreover, each peak reflects specific cellular and biochemical processes [40]. MR images obtained in a patient with normal brain tissue are shown in Fig. 1*a* and the image of MRS signal obtained in a 22 years old biopsy-approved male with a grade IV glioblastoma multiform (GBM) brain tumour are denoted in Fig. 1*b*. When the spectrum of glioblastoma brain

Table 1 Peak values and characteristics of significant ^{1}H-MRS metabolites of human brain in short TE

ppm range/peak value (63 MHz)	Metabolite/spectral assignment	Observable properties
0.9–1.3	macromolecules, amino acids, lipids (Lip)	disintegration of brain tissue
1.35	lactate (Lac)	anaerobic glucose marker
1.47	alanine (Ala)	occurs in ABC and MEN
1.9	acetate (Ace)	visible with ABC
2.02, 2.6	NAA	symptoms of neuron health/neural marker
2.05/2.5	glutamate + glutamine (Glx)	neuro-transmitter
2.4	pyruvate (Pyr), succinate (Succ)	in case of pyogenic ABC
3.02, 3.9	creatine (Cr)	cell metabolism, cell proliferation
3.2	choline (Cho)	cell metabolism, cell proliferation
3.36	scyllo-inositol and taurine (Tau)	visible in cases of PNET and some gliomas
3.56, 4.06	myo-inositol (mI), glycine (Gly)	osmotic marker, recommended glial marker

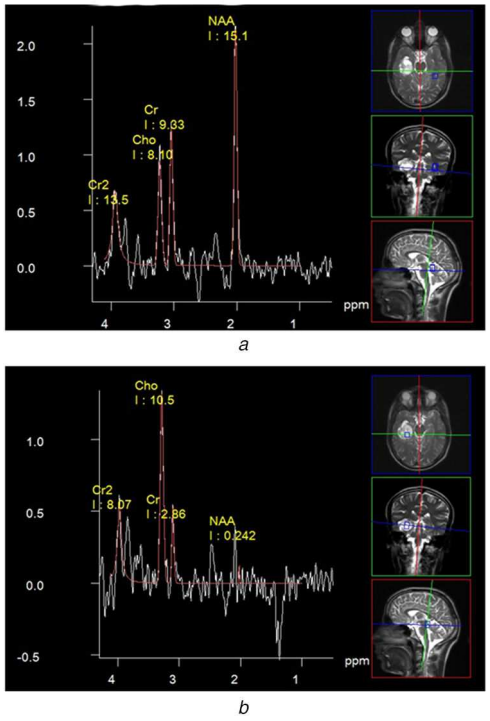

Fig. 1 *MRS signal patterns for patients with normal brain tissue and glioblastoma brain tumour*
(a) MRS of a patient with normal brain tissue, ***(b)*** MRS of a patient with glioblastoma

tumour lesion in Fig. 1*b* and the spectrum of normal brain tissue given in Fig. 1*a* are examined, the increase in Cho/Cr ratio, the excess increase in Cho/NAA ratio, and the excess increase in Lac/Cr ratio are observed. Consequently, these findings indicate that this case could be probably a high-grade glioma.

3 Material and method

In this study, MRS signal data were used for classification of brain tumours. In order to obtain classification results for pattern recognition techniques, a feature extraction method called as aiMRS on MRS data was proposed. The processing steps of the proposed method are shown in the scheme in Fig. 2, respectively. The proposed system consists of six steps. First, the MRS data is acquired using an MR scanner and then the biopsy verification is approved after obtaining MRS data. Afterwards, the spectra are pre-processed and the peak is integrated within each voxel for raw MRS signals. For classification, relevant features are extracted from processed signals using aiMRS method proposed in this study. Finally, MRS signal patterns are classified using several pattern recognition methods.

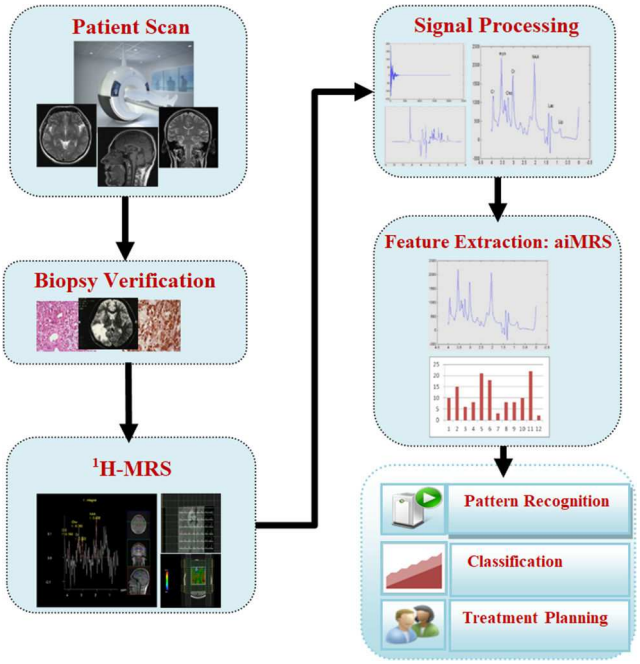

Fig. 2 *General block scheme showing the steps of the proposed method*

3.1 MRS data set and protocols

The MRS data used in this study were obtained with special permission from the database of international INTERPRET project [41]. The INTERPRET project is a multicentre project and the data collected at six different centres such as the Center Diagnostics Pedralbes (CDP) from Barcelona, Spain; St. George's Hospital Medical School(SGHMS) from London, UK; Fundacíon para la Lucha contra las Enfermedades Neuroĺogicas de la Infancia (FLENI) from Buenos Aires, Argentina; Institut de Diagnostic per la Imatge (IDI) from Barcelona, Spain; University Medical Center Nijmegen (UMCN) from Nijmegen, The Netherlands and Uniwersytet Medyczny w Lodzi (MUL) from Lodzi, Poland. Scanning of the patients was performed with Siemens, General Electric and Philips MRI scanners. The data acquired from MRS signals between 1994 and 2001 were recorded in the database. The signals were obtained at 1.5 T short TE (20–32 ms) Point-resolved spectroscopic sequence (PRESS) and Stimulated echo acquisition mode sequence (STEAM) acquisition sequences, both with and without water suppression. The database includes 257 short TE MRS data. The spectral parameters were determined as repetition time (TR) = between 1600 and 2020 ms, TE = between 20 and 30–32 ms. In addition, spectral width was between 1000 and 2500 Hz and was selected as 512, 1024 or 2048 data-points. All MRS data in the database were classified in accordance with classification principles of the central nervous system tumours determined by the World Health Organization [42].

In the project infrastructure, there are MRS signals belonging to many brain tumour types. The voxel selections for each patient was

Table 2 Detailed information and number of data for short TE ^{1}H-MRS obtained from data centres

Data centre	Acquisition type	Number of cases								Total
		GBM	MEN	MET	DAST	PAST	AAST	NOR	ABS	
CDP	STEAM	30	12	5	4	2	0	4	2	59
SGHMS	STEAM	12	4	5	6	0	4	5	0	36
	PRESS	6	8	11	4	0	3	7	0	39
FLENI	PRESS	2	0	0	1	0	0	0	1	4
IDI	PRESS	31	30	17	5	1	3	5	5	97
UMCN	STEAM	2	1	0	1	0	0	10	0	14
MUL	STEAM	4	2	1	1	0	0	0	0	8
total		87	57	39	22	3	10	31	8	257

input : $Self_{set}$ = set of seen known self elements (training set)
output : A: Abnormal set generated from $Test_{set}$, N: Normal set generated from $Test_{set}$
D = Generated detector set, P: Candidate detector set, $Test_{set}$: Test set,
begin
while (Stopping criteria)//Training phase
Randomly generating potential/candidate detectors and placing them in *P* set
Determining the affinity of each member of *P* with each member of the $Self_{set}$
Adding the candidate detector in the P set to the D set that matches the $Self_{set}$ according to the training-detector threshold value, and rejecting the non-matched ones
end
while (Stopping criteria)//Test phase
Determining the affinity of each member of *D* with each member of the $Test_{set}$
Marking patterns in $Test_{set}$ set as 'Normal' matches D set the according to the test-detector threshold value, and marking as 'Abnormal' the non-matched ones
end
end

Fig. 3 *Procedures of NSA and expression of it's algorithm with pseudo code*

performed and validated by the experienced experts in INTERPRET project committee. In this study, GBM, MEN, MET, pilocytic astrocytoma (PAST), diffuse astrocytoma (DAST), anaplastic astrocytoma (AAST), normal brain tissue (NOR) and ABC obtained for ^{1}H-MRS data were used and detailed information about the data are given in Table 2.

3.2 Artificial immune system

AIS is a method developed by inspiration of the natural immune system in living organisms. AIS was proposed for the solution of problems in mathematics, engineering and information technologies [43]. It has a complex structure due to its abilities such as learning, memory and detection of new situations. Therefore, it is used in many application areas such as error detection, pattern recognition, anomaly detection, classification [44]. There are various algorithms developed in AIS. However, the most commonly used AIS algorithms are NSA and CSA. While NSA is generally used for anomaly detection, CSA is used for optimisation problems. In this study, for feature extraction from MRS signals, NSA was used to determine activated detectors and CSA was used to adaptively determine the threshold values between training/test sets and detector set.

3.2.1 Negative selection algorithm: Inspired by the negative selection feature of the human immune system, the NSA was proposed by Forrest *et al.* [45] for the detection of abnormal and changing conditions. This algorithm is able to detect abnormal data through the generated detectors. Different types of NSA methods proposed and characterised in the literature such as feature representation schemes, matching rules and detector generating processes [46]. In the training phase of the NSA, first of all, candidate detectors are generated randomly. A procedure is then performed by checking whether the detector set and the training (self-set) set are matched according to the specified threshold value [47]. During the training phase, if a detector matches with a sample in the training set, then it is eliminated. Detectors which are not recognised are added to the mature detector set and the training phase is completed. In the testing phase, an input data in self-set is compared to each sample in the detector set. After this process, the data is classified either as normal or abnormal data depending on the matching.

The pseudo-code of NSA algorithm is denoted in Fig. 3. The generation of detectors in the NSA is initialised with a candidate detector population through an iterative process. Then, the distance of each candidate detector with the self-set is calculated for each iteration and the matched ones are rejected. The non-self-detector sets are then stored and ranked according to their distance. The detectors with larger distance (and smaller overlap with other detectors) are considered as better-fit and selected to go to the next generation. However, detectors with very small distance are replaced by the clones of better-fit detectors.

3.2.2 Clonal selection algorithm: The clonal selection principle is used to explain the basic features of an adaptive immune response to an antigenic stimulus [48]. This principle emphasises the idea that only cells that recognise antigens proliferate. The selected cells are subject to an affinity maturation process, which improves their affinity to the selective antigens [49, 50].

The steps of the CSA can be described as follows. In order to show the A_g antigen set and the A_b antibody set:

(i) A random set of antigen (A_{gi}) is generated and all are represented in the set (A_b) of the antibody. Here, it can be seen that A_b = memory cells (A_{bm}) + remaining cells (A_{br}) = A_g.
(ii) The matrix (f_i) of all N patterns in the A_b set is determined from the fitness values calculated according to the affinity measurement with the A_g set.
(iii) In the As_b set, n with the highest affinity A_b is selected and the A_{bn} set is created.
(iv) The selected Ab's are independently cloned (re-generated) according to their antigenic compatibility and the set (C_i) containing the cloned cells is formed. The cell with the highest antigenic compatibility is further cloned. Equation (1) is used for cloning. In this equation, N_c represents the total number of clones for each antigen, β is the cloning factor and N is the total number of antibodies (if the multiplication of the cloning factor and antibody number is not an integer, the rounding function is used to determine the number of antibodies to be cloned)

$$N_c = \sum_{i=1}^{N} \text{round}(\beta . N) \quad (1)$$

(v) Cells in the cloned C_i set are mutated inversely according to their antigenic compatibility and form the set (C_i*) in which the mutated cells are located. The cell with the highest fitness has the smallest mutation rate. Thus, this cell is the least modified cell. Each cell mutates according to the expression in (2). In this expression, α mutation rate, ρ mutation factor and f are affinity

measurements (exp in the equation is the number of natural logarithms).

$$\alpha = \exp(-\rho \cdot f) \quad (2)$$

(vi) The affinity values (f_i*) of each cell in the cluster of C_i* cloned cells are calculated in relation to the cells in the A_g antigen set.

(vii) The highest suitability A_b from the matured C_i* set is re-selected. If the suitability of this cell is better than the same row cell in the A_b memory cell set, it is replaced.

(viii) Finally, d from A_{br} to the lowest suitability cell is replaced with d new cells in the A_{bd} set and diversity is achieved.

3.3 MRS signal pre-processing

In this study, each MRS signal is processed according to the protocols specified in the INTERPRET [32] project. The following steps are followed in order to automatically pre-processing of MRS signals of all cases in the database [13]:

(i) Eddy current correction is applied to water-suppressed free induction decay of each case using Klose algorithm [20].

(ii) The residual water resonance is removed using the Hankel–Lanczos singular value decomposition time-domain selective filtering using ten singular values and a water region of [4.33, 5.07] ppm s

(iii) A Lorentzian function of 1 Hz of damping is applied to eliminate the signal damping.

(iv) Before transforming the signal to the frequency domain using the fast Fourier transform, an interpolation is needed in order to increase the frequency resolution of the low resolution spectra to the maximum frequency resolution used in the acquisition protocols. This is carried out with the zero-filling procedure.

(v) Then, the baseline, which is estimated to occur as the mean value of [9, 11]∪[−2, −1] ppm, is subtracted from the spectrum.

(vi) The normalisation of the spectral data vector is performed based on the data-points in the region [−2.7, 4.33]∪[5.07, 7.1] ppm.

(vii) Depending on the signal-to-noise ratio and the tumour pattern, an additional frequency alignment is performed for spectrum control by referencing the ppm-axis to the tCr at 3.03 ppm and to the tCho at 3.21 ppm and at 1.29 ppm.

(viii) Finally, the region of interest is restricted to [0.5, 4.1] ppm in order to obtain a vector of 190 points for each spectrum.

The pre-processing steps of the MRS signal obtained from a brain tissue are denoted in Fig. 4. The time-amplitude of the signal obtained at TE = 20 ms is shown in Fig. 4*a*. Here, this is raw data and contains 2048 samples. In addition, re-sampled form of the MRS signal is shown as 512 samples in Fig. 4*a*. The graph of this signal in the frequency-amplitude plane in Hz scale is shown in Fig. 4*b*. Since this signal is difficult to interpret, this graph is obtained by re-sampling on the ppm frequency scale. As seen in Fig. 4*b*, it is seen that when MRS signals are converted from time domain to frequency domain, positive and negative frequencies are formed. Here, when the Fourier transform applies to signal, some resonances can appear between positive peaks and negative peaks. In order to fix this, a phase correction can be applied to the whole spectrum of the signal by multiplying the spectrum. Thus, all peaks can be corrected to positive [51]. The corresponding metabolites of the signal are set at 0–4 ppm scale in Fig. 4*c* as spectral values appeared between 0 and 4 ppm. For this signal, which occurs in the range of 0–4 ppm, the ppm value and signal densities at which metabolites appear are shown here.

3.4 Feature extraction from MRS data

^{1}H-MRS can be used as a powerful non-invasive tool for the classification or grading of brain tumour, when combined with robust and reliable classification techniques. An important step in classification strategies is the selection of the input space. When MRS data are considered, input data used in combination with pattern recognition techniques can be generated both as a full spectrum (FS) and as a set of features extracted from the spectrum.

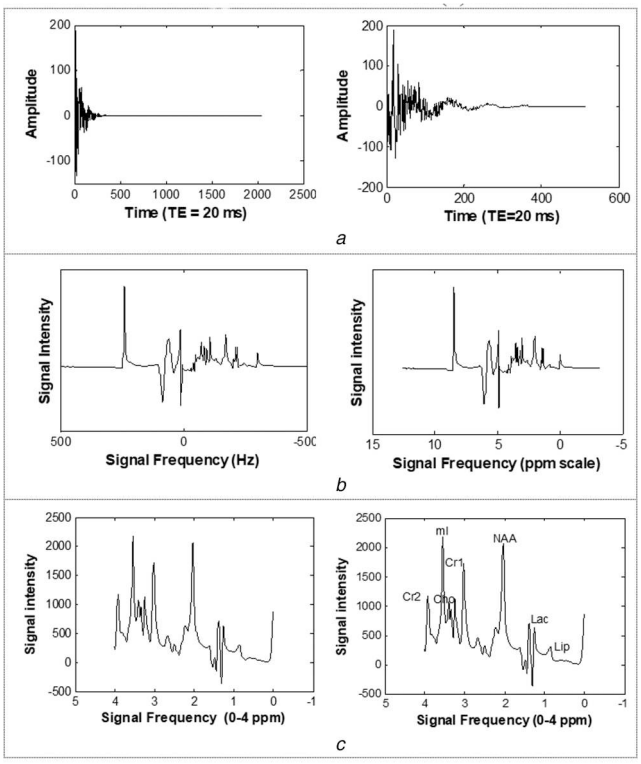

Fig. 4 *Representation of normal brain ^{1}H-MRS time, frequency, ppm and metabolites*

(a) Display of signal in amplitude-time plane and receiving the portion of interest of the raw signal, ***(b)*** Display of signal in frequency-amplitude plane and signal conversion to ppm frequency scale, ***(c)*** Display of the signal in the 0–4 ppm frequency range and display of metabolites in ppm range

A metabolic data of interest can be considered as extracted features based on biochemical relationships in classification problems. Pattern recognition in MRS signals is based on all spectrum values of the signal or on the basis of selecting some spectral values using feature extraction methods. However, instead of using the whole spectrum information, selecting the characteristics of the important frequency regions provides more successful results. In the literature, several feature extraction methods have been proposed to detect tumours from MRS signals. Some of these methods are peak integration (PI) [52–54], peak region selection [28, 53], principal component analysis (PCA) [53, 55, 56], independent component analysis (ICA) [53, 57] and wavelet transformation [58]. In some studies, all data regions of the signal (FS) are used at 190 or 138 ppm (between 0 and 4.17 ppm) as a feature [53, 59]. In addition, in some studies the metabolite features of MRS signals are extracted using feature selection methods such as relief-F, kruskal–Wallis and fisher criteria. There are also model-based methods such as AQSES, QUEST for feature extraction from MRS signals [60].

In this study, popular feature extraction methods such as FS, PI and PCA, which are the previously proposed feature extraction methods and the proposed feature extraction method (aiMRS), were used for feature extraction from MRS signals. In FS, the whole 190 points, which correspond with a region of interest of [0.0–4.17] ppm MRS frequency spectrum, are retained for full spectra. PI is used to extract significant features for selection of important peak values and obtain measures for brain metabolites. For MRS data set, 13 peak values are determined based on MRS spectrum such as Cr1, Glx1, Tau + Glc, mI + Gly, mI + Tau, Cho, NAA, Ala, Lac, Lip1, Cr2, Lip2, Glx2 as reported in [54]. PCA transforms the original features to new set of uncorrelated features. The transformation provides a mapping of the vectors to low dimensional vectors. These new features are linear combinations of the original variables and they are often ranked according to the variance [60]. For comparison of the feature extraction methods, the first 13 principal components are selected for the MRS data set.

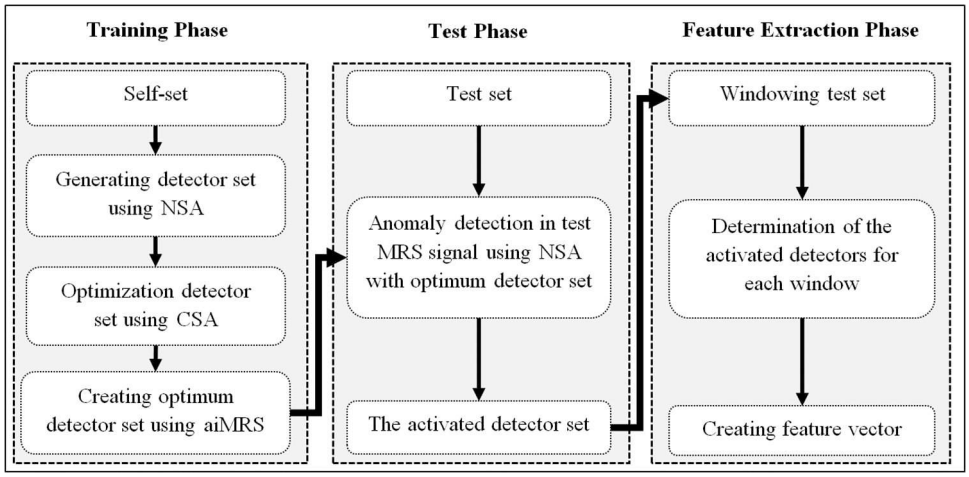

Fig. 5 *Flowchart of the proposed feature extraction method using aiMRS which consist of three phase such as training, test and feature extraction phases*

3.5 Pattern recognition methods for MRS signal classification

In this study, probabilistic neural networks (PNNs), extreme learning machine (ELM), SVMs, LDA, Bayes classifier and *k*-nearest neighbour (*k*-NN) algorithm methods, which are among the pattern recognition methods used for classification, were used for the classification of MRS signals. In addition, the comparative analysis of these classification techniques was performed on the results in terms of several performance measurement metrics.

PNN is a model of artificial neural networks used in probabilistic classification [61]. It is an effective tool for many classification applications since it has Bayesian theory and easy classification [62]. PNN uses the probability density function format, which is also found in some classification methods, for checking the structure of the network. The pdf structure that requires the use of Parzen windows works according to Bayesian decision theory [63]. In this study, the smoothing parameter for PNN was defined as 1.

ELM is feed-forward neural network and has a single hidden layer [64, 65]. In ELM, the input weights are randomly chosen without updating, while output weights are assigned analytically. Therefore, the training speed of ELM can be faster than traditional ones [66]. The gradient-based learning algorithms used in neural networks aim to reach minimum training error without considering the magnitude of weights, but ELM intends both reaching minimum training error and obtaining the smallest weights. Thus, ELM tends to have better classification performance [64]. In this study, the number of cells in the hidden layer for ELM was 1000 and the activation function was sigmoidal.

The Bayesian classifier solves classification problems statistically and is based on the Bayes decision rule [67]. In the Bayesian classifier, the information on which data belongs to which class is a determined probability. In this equation, (C_1, C_2, …, C_n) denotes n classes and $X_k = [x_1, x_2, \ldots, x_k]$ shows k feature vector. Thus, $p(C_i \mid X_k)$, Bayes rule showing the probability that X_k belongs to class C_i is denoted in (3). In this study, the data set consists of numerical attributes, the Gauss distribution was used to calculate probabilities for Bayesian classifier

$$p(C_i \mid X_k) = \frac{p(X_k \mid C_i)\, p(C_i)}{p(X_k)} \qquad i = 1, 2, \ldots, n \tag{3}$$

SVM is one of the effective learning methods used in classification problems [68]. SVM is successful classifiers developed to separate the input data into two categories. A SVM classifier helps to obtain the best separator linear line equation for splitting an input data set into two categories [69]. SVM uses kernel functions to classify larger data [70]. The classification success of SVM depends on the selection of the best kernel function [71]. SVM works well on the data sets that have a large number of attributes. However, these data sets have to include in a small number of data. [72]. In this study, radial basis kernel function was used SVM classifier.

k-NN decision rule is a non-parametric supervised pattern classification method [73]. In this method, the affinity of the data to be classified to the normal data sets in the training set is calculated, and classification is performed according to the threshold value obtained by averaging the k data which is considered to be the nearest [74]. Before classifying, the features of each class have to be specified clearly. In this study, *k*-value and distance measurement method for *k*-NN are determined as 2 and Euclidian, respectively.

LDA is basically a method that converts data from the original input space into a one-dimensional (1D) variable and provides the distinction between them using these variables. That is, it is used to reduce and separate data from high to lower dimensions [75, 76]. Owing to this feature, it is preferred in the classification of data. This method shows more successful results in binary classification problems.

4 aiMRS: proposed feature extraction method on MRS data

In this study, a hybrid method named as aiMRS based on CSA and NSA algorithms of AIS was proposed for feature extraction from MRS signals before classification step. In the aiMRS, the NSA was used to identify activated detectors, while the CSA was used to determine threshold values between training and test data and detector sets as heuristic.

The hybrid aiMRS method proposed in this study was performed in three stages as shown in Fig. 5. First, in the training phase, a training signal was specified from the MRS data set and the detector set was created using NSA according to this set. The detector set was then optimised using the CSA to adjust the most suitable detector set. In the second step, a test signal was used to determine the optimal detector set and the detectors activated according to the NSA. In the feature extraction stage, which was the last stage, the activated detectors are applied to the windowed test signal according to the sliding window method, and then a feature vector was obtained. This vector was used for the classification of the signals in the next stage.

4.1 MRS signal training phase

In order to detect abnormal changes in MRS signals, first of all, training phase is required. The first step of the training phase is specifying the training signals for the NSA. MRS training signals are preferably selected from data of cases such as normal brain tissue, MEN, GBM and astrocytoma. The pre-processed MRS signals are shown in Fig. 6 and these signals are used as training data. After specifying the MRS training signal, the training procedure of this signal is performed according to the rules of the NSA algorithm, and therefore the candidate detector set is created.

In the second stage of the training phase, a detector set is created using the NSA algorithm. For this, the self and non-self differentiation principle of the NSA algorithm is used. According

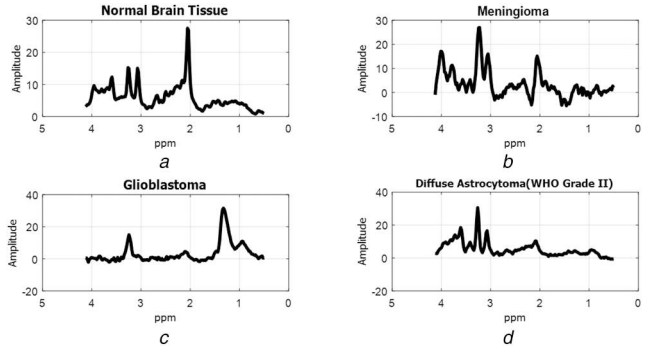

Fig. 6 *Sample MRS signal patterns used for training*
(a) Normal brain tissue, ***(b)*** MEN, ***(c)*** Glioblastoma, ***(d)*** DAST

to this principle, distance measurement is performed by Hamming affinity measurement between the each sample in the detector set and in the training set. According to a specified threshold, candidate detectors matching the training set are removed and replaced by new ones, while detectors that do not match the training set are added to the mature detector set. These processes continue until the number of detectors that need to be generated in the system is reached.

In MRS signal training phase, the number of detectors was determined as 50 and the number of iterations was determined as 500. The candidate detectors and detector set of a MRS signal (blue colour signal) of normal brain tissue obtained according to these values are shown in Fig. 7. The candidate detectors (pink colour points) generated for the MRS signal of the normal brain tissue used for the training signal are shown in Fig. 7*a* and the detector set generated using the NSA for the same training signal are shown in Fig. 7*b*.

As can be seen in Fig. 7*b*, the detector set generated by the conventional NSA algorithm does not fully coincide with the signal. That is, a weaker detector set is occurred. This restrictive situation would result in lower detection performance during the classification stage of the MRS signal and the feature extraction stage. Therefore, the generated detector set is optimised using CSA to create the most suitable detector set. To figure out fitness (f) in the optimisation procedure by CSA, the function shown in (4) is used. Accordingly, the fitness value f for CSA is calculated according to whether a detector is equal to or greater than the difference between the average of each pattern in the training set S and each pattern in the average of the T test sets

$$f = \frac{1}{n}\sum_{i=1}^{n} S(i) - \frac{1}{n}\sum_{i=1}^{n} T(i) \tag{4}$$

where f represents the fitness value for CSA, S represents the training set, T represents the test set and n represents the sample number in the training and test sets. The detector set generated by using classic NSA for normal brain tissue is presented in Fig. 8*a* and the detector set optimised by using CSA is presented in Fig. 8*b*. Accordingly, it is seen that the CSA-optimised detectors seem to overlap (match) more with the MRS signal. Therefore, the training stage of the feature extraction stage is completed successfully.

4.2 MRS signal test phase

The first step in the test phase is to determine the test MRS signal. Preferably, after a training signal is specified, a test signal is also selected to reveal errors, abnormalities, rising or falling peaks in the signal. A training signal of normal brain tissue loaded into the system (blue colour) and a test signal of a patient with GBM brain tumour (red colour) are denoted in Fig. 9*a*.

The next step after determining the test signal is to detect abnormal changes in the test signal using the training signal. For this purpose, the principle of identifying non-self-patterns of the NSA is used. A match is occurred between the most suitable detector set determined by CSA and the test set according to a

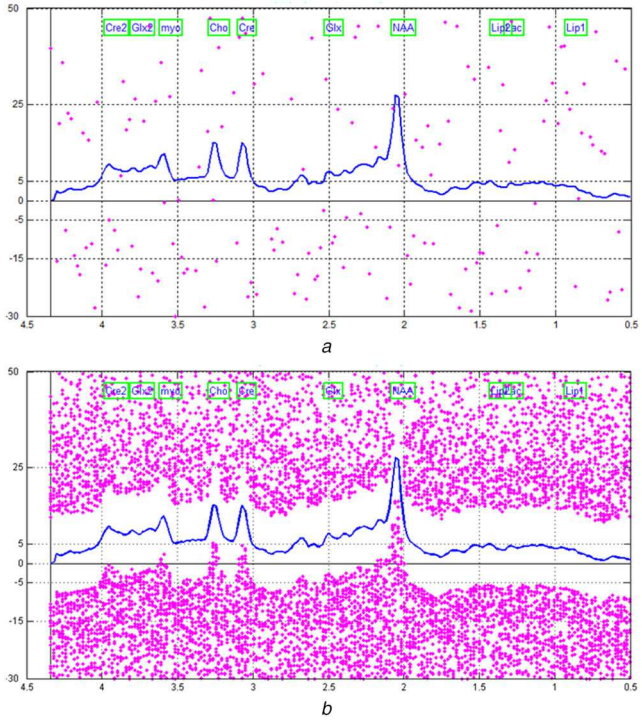

Fig. 7 *Candidate and mature detector sets generated using NSA*
(a) Set of candidate detector generated with NSA, ***(b)*** Set of detectors generated with NSA

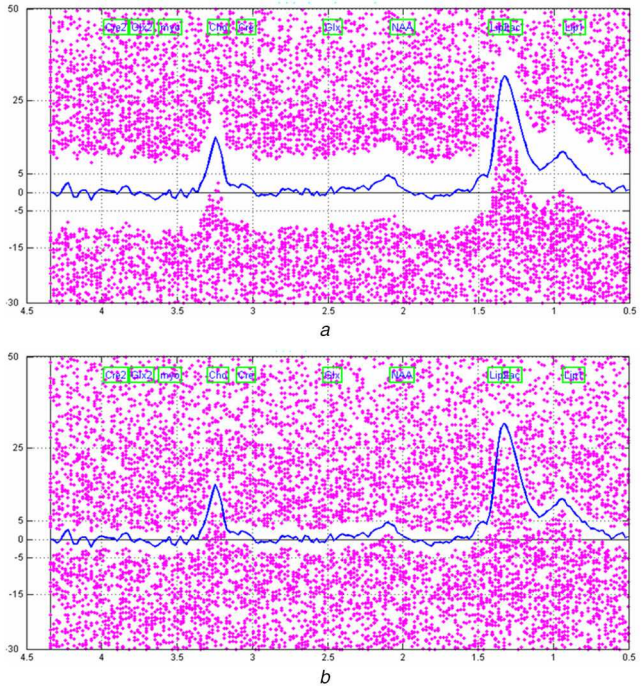

Fig. 8 *Optimising the detector set with CSA and generating optimum detector set*
(a) Set of detectors generated with NSA, ***(b)*** Optimal detector set optimised with CSA

threshold value determined by Hamming affinity measurement and NSA. As a result of this match, each sample in the test set that matches the detector set is identified as abnormal. The detectors that enable matching in the test set are called as activated detectors. The more the detector is activated during the evaluation of the signal, the more errors are considered in the signal. Therefore, the ratio of activated detectors is the fundamental criterion used to measure the error in the signal. The abnormalities on a test signal are shown in Fig. 9*b*. These abnormalities are determined according to the activated detectors. The blue signal is the training signal, showing the MRS signal of a normal brain tissue and the

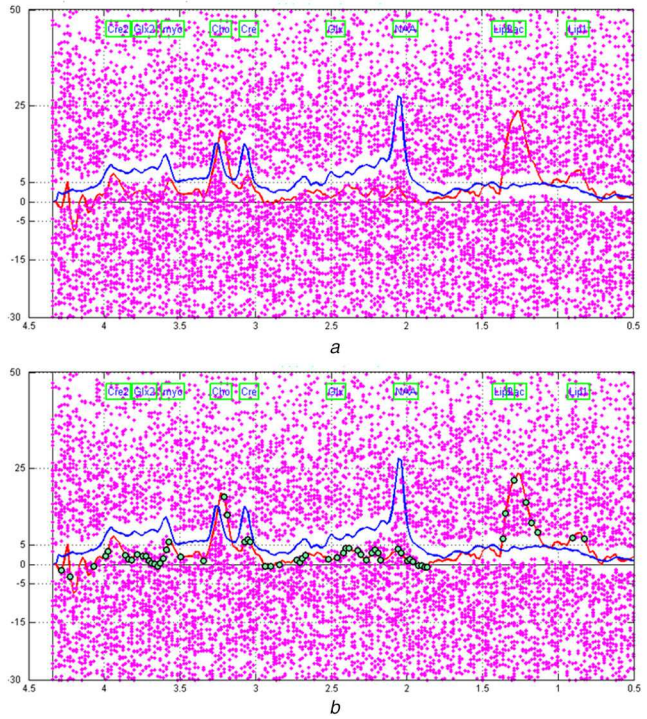

Fig. 9 *Determination of the MRS test signal for the proposed system and detection of anomalies in the MRS test signal using the activated detectors*
(a) Determination of MRS test signal pattern, ***(b)*** Determination of anomalies in the MRS test signal

red signal indicates the test signal, showing the MRS signal of a patient with GBM brain tumour. The green dots on the test signal denote abnormal areas in the test signal relative to the training signal. The threshold value used during the affinity distance measurement between the test signal and the detector set is again determined according to the CSA algorithm. This threshold value is determined to make the affinity measurement between the test set and the detector set greater than the average value of the test signal and nearest to the test signal. Thus, this threshold value is determined as adaptive (heuristic).

4.3 Feature extraction phase on MRS signals

At this stage, the first step of feature extraction is performed. After detecting abnormal conditions in the test signal, the activated detectors in each window are calculated by sliding the signal into windows. In this study, classification of MRS signals consisting of 190 points according to all points may not produce successful results. Instead, the signal is subdivided into equal windows of 10 points to extract its features for covering each metabolite in the ppm frequency spectrum of the MRS signal. Thus, the change in each metabolite is measured. Afterwards, the feature extraction is performed by sliding between the windows and determining the sum of the activated detectors in each window. The activated detectors in each window of a test signal are shown in Fig. 10*a* and the number of activated detectors in each window of the test signal is shown in Fig. 10*b*.

The next stage after determining abnormal conditions and the activated detectors in the test signal is the feature extraction stage. At this stage, instead of using all values of MRS signals consisting of 190 points, a smaller number of input data is used by extracting a feature from the activated detector numbers. The MRS signal is processed through several stages according to the method called as aiMRS and features are created. In the windowing, as shown in Fig. 11, a 190-bit binary sequence is first generated to match the 190 points of the test signal. Therefore, at each point of the test signal, if the detector is activated, depending on its activation, bit values of element of this sequence is assigned as 1, else assigned as 0, respectively. This binary array is then divided into a total of 19 equal windows consisting of 10 points. After this process, the total number of activated detectors in each window is calculated, the

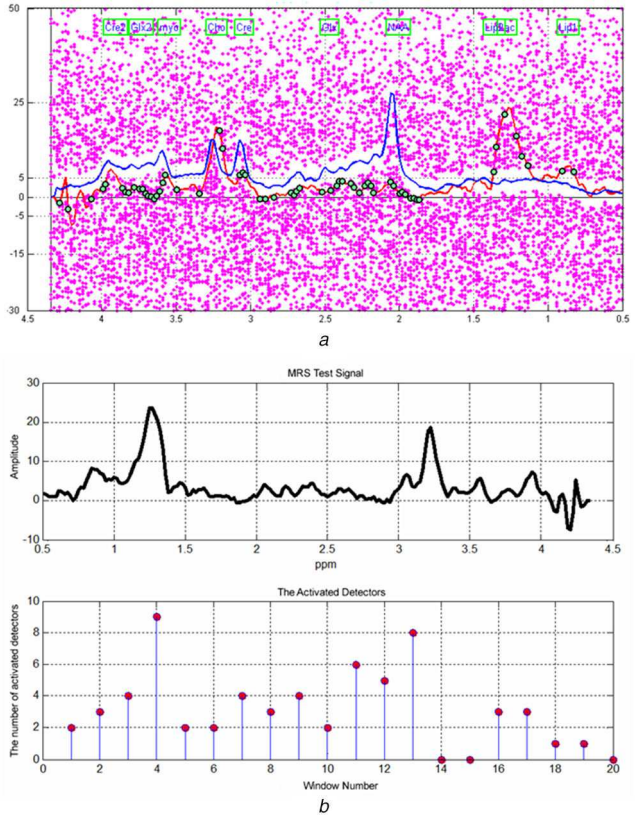

Fig. 10 *Activated detectors in test signal and number of detectors activated by window numbers*
(a) Activated detectors in test signal, ***(b)*** Activation number of detectors by windows

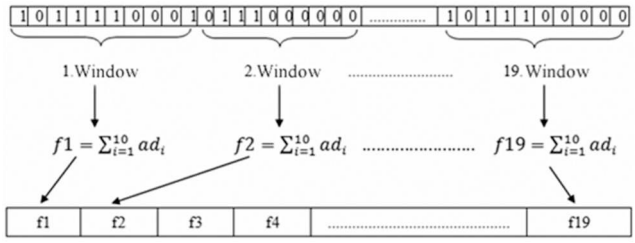

Fig. 11 *Feature extraction from MRS signals using the proposed aiMRS method*

obtained values are assigned to a sequence of feature containing 19 decimal values as $x = [f_1, f_2, \ldots, f_{19}]$. Therefore, the measurement of the change in each metabolite is performed and then feature extraction using aiMRS is completed.

5 Results

In this study, experimental studies were performed by three different experiments to measure the performance of aiMRS which is AIS-based feature extraction method to be proposed for the classification of brain tumours on MRS signals. These experiment tasks include the classification of normal brain tissue and tumour brain tissue, differentiation of benign and malignant tumours and the distinction of primary brain tumours and metastatic brain tumours. All experimental studies were carried out on the application with the user interface created with MATLAB software using a computer with configurations presented in Table 3. DSS software [77] was used to convert the raw MRS signals obtained from the INTERPRET database into ppm frequency spectrum data. Software used for all other processes was developed specifically for this study.

In the experimental studies, the performance results of classifiers were obtained after the feature extraction was performed using proposed aiMRS method. The classification results based on aiMRS were compared with the results acquired by the popular

feature extraction methods from MRS signals. FS, PI and PCA are the other feature extraction methods used for making comparison with the aiMRS. Six methods were applied to obtain the classification results. These methods included PNN, ELM, SVM, Bayes, LDA and *k*-NN. In addition, accuracy, sensitivity, specifity, positive decision value (PDV) and negative decision value (NDV) performance measures were figured out to evaluate the detection performance of the proposed method. Equations used in the calculation of these criteria according to true positive (TP), true negative (TN), false positive (FP) and false negative (FN) values are presented in the following list

- Accuracy (ACC): (TP + TN)/ (TP + TN + FN + FP)
- Sensitivity (SEN): TP/(TP + FN)
- Specifity (SPE): TN/(FP + TN)
- PDV: TP/(TP + FP)
- NDV: TN/(TN + FN)

It is difficult to precisely determine the amount of density of metabolites in nuclear MRS. For this reason, the intensity value of the signal of interest is defined as a ratio of the integral of the metabolite signal above the total spectrum. Therefore, the peak value of each signal is normalised according to the total spectrum value. This final value is also used for statistical analysis evaluation. In this study, the ratios of the significant metabolites in MRS signal for brain tumours to Cr peak formed at 3.93 ppm were analysed and evaluated using Statistical Package for Social Science(SPSS) program. Significant changes in metabolite levels were considered statistically significant at $p < 0.05$. In addition, 95% confidence interval analysis was performed for the reliability test in the classification of data.

Table 3 Hardware specification of the computer used for the experimental studies

Hardware	Configurations
processor (CPU)	Intel Core i7-7700 K @ 2.8 GHz (8 CPUs)
memory (RAM)	16 GB (DDR4 2400 MHz)
mainboard	ASUS X580VD
GPU	NVIDIA GeForce GTX 1050 (4 GB)
harddisk drive (HDD)	256 GB SSD HDD

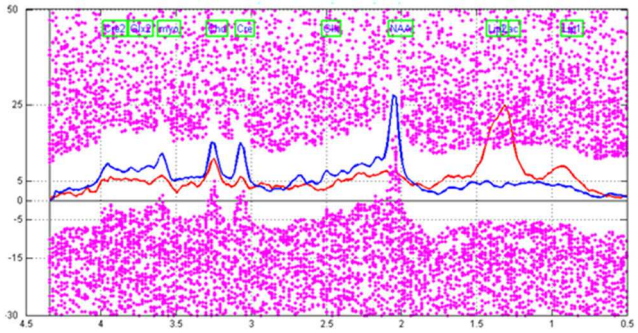

Fig. 12 *Training and test MRS signals for the differentiation of normal brain and GBM brain tumours and metabolite changes according to detector set*

In order to test the performance and to determine the parameters of the classifiers, leave-one-out cross validation (LOOCV) method was used for the experimental studies. LOOCV is a special type of *k*-fold cross validation. In LOOCV, *k* equal to the number of data in the data set. LOOCV uses the entire data set both in training and testing phases of the classifier. LOOCV was performed on a set of each classification procedure. Each classifier was validated using single MRS data and trained on the remaining data. This process was repeated until each image in the set was used once as the test data. The confusion matrix values for experiments in this study were obtained as the average values of the classifier after all iterations.

In the experiments, the number of components such as 5, 10, 12, 15 and 20 for PCA was selected and the results of the classifier were tested. The most successful results were obtained when the first 12 components were selected for PCA. However, for another feature extraction method PI, 13 peaks were determined and tested. In order to compare the results with the same parameter numbers, the first 13 components were obtained for PCA and the performance of the classifiers was tested.

In the first experiment, in order to differentiate normal brain tissue and tumour cases, MRS signals obtained from patients with normal brain and GBM brain tumour were tested with different feature extraction methods and classifiers. MRS signal pattern of 30 cases for normal brain and 85 GBM signal pattern for tumour cases were used in this experiment. The values of the metabolites obtained from normal brain tissues and GBM tumour tissues and sample MRS signals are denoted in Fig. 12. When the most important differences between the two tissues are examined, it is seen that there is an excessive increase in Lac + Lip peaks which appear in the frequency ranges of 1.3–1.4 ppm, and an excessive decrease in NAA peak, which is observed at a frequency value of ~2.02 ppm.

The confusion matrix showing the results obtained from the detailed experiments performed for the differentiation of normal brain tissue and tumour cases is presented in Table 4 and the analysis of the performance criteria are presented in Table 5. When the results of this experiment for the normal brain tissue and GBM brain tumours are examined, it is seen that very successful results are obtained as 100% ACC when the feature extraction is performed by aiMRS method and classification is performed. Furthermore, when ELM, LDA, SVM and PNN classification methods are used, it is seen that all cases are successfully differentiated. In addition, if aiMRS is selected as feature extraction method in this experiment, more successful results are obtained by several classifiers for other performance metrics such as SEN, SPE, PDV and NDV. On the other hand, in this experiment, all of MRS signals for 85 GBM cases and 30 normal brain tissues are classified truly using ELM, LDA, SVM and PNN classifiers with aiMRS feature extraction method, proposed in this study.

In the second experiment, another test procedure was performed to differentiate benign and malignant brain tumours using MRS spectrum data. In the experiment, as in the differentiation of normal brain tissue and brain tumours, different feature extraction methods and classifiers and experimental tests were performed and performance comparisons of these methods were conducted. Here, MRS signals of GBM type brain tumours for 85 cases and MRS signals of MEN type brain tumours for 56 cases were used to differentiate benign from malignant brain tumours. As seen in

Table 4 Obtained confusion matrix using feature extraction and classification methods for the differentiation of normal brain tissue and brain tumours in the first experiment

Classifier	TP				FP				FN				TN			
	FS	PI	PCA	aiMRS	FS	PI	PCA	aiMRS	FS	PI	PCA	aiMRS	FS	PI	PCA	aiMRS
PNN	71	80	78	85	0	0	0	0	14	5	7	0	30	30	30	30
ELM	77	81	79	85	0	0	0	0	8	4	6	0	30	30	30	30
SVM	76	81	76	85	0	0	0	0	9	4	9	0	30	30	30	30
LDA	75	78	77	85	0	0	0	0	10	7	8	0	30	30	30	30
k-NN	70	75	76	80	0	0	0	0	15	10	9	5	30	30	30	30
Bayes	68	73	71	76	3	1	2	0	17	12	14	9	27	29	28	30

Table 5 Performance comparisons of obtained classification results for differentiation of normal brain tissue and brain tumours in the first experiment

Classifiers	Performance metrics																			
	ACC				SEN				SPE				PDV				NDV			
	FS	PI	PCA	aiMRS	FS	PI	PCA	aiMRS	FS	PI	PCA	aiMRS	FS	PI	PCA	aiMRS	FS	PI	PCA	aiMRS
PNN	87.83	95.65	93.91	100	83.53	94.12	91.76	100	100	100	100	100	100	100	100	100	68.18	85.71	81.08	100
ELM	93.04	96.52	94.78	100	90.51	95.29	92.94	100	100	100	100	100	100	100	100	100	78.95	88.24	83.33	100
SVM	92.17	96.52	92.17	100	89.41	95.29	89.41	100	100	100	100	100	100	100	100	100	76.92	88.24	76.92	100
LDA	91.30	93.91	93.04	100	88.24	91.86	90.51	100	100	100	100	100	100	100	100	100	75.0	81.08	78.95	100
k-NN	86.96	91.30	92.17	95.65	82.35	88.24	89.41	94.11	100	100	100	100	100	100	100	100	66.67	75.0	76.92	85.71
Bayes	82.61	88.70	86.09	92.17	80.0	85.88	83.53	89.41	90.0	96.67	93.33	100	95.77	98.65	97.26	100	61.36	70.73	66.67	76.92

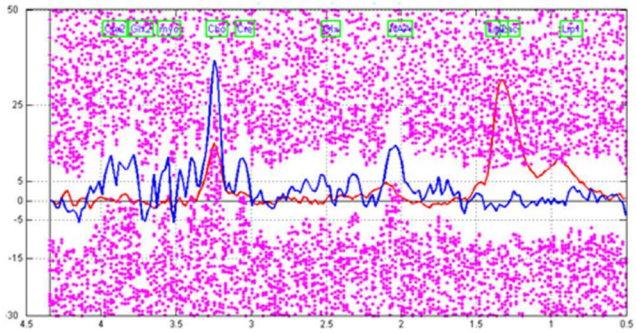

Fig. 13 *Training and test MRS signal patterns of MEN and GBM, respectively, for the differentiation of benign and malignant brain tumours*

Table 6 Obtained confusion matrix using feature extraction and classification methods for the differentiation of benign and malignant brain tumours in the second experiment

Classifier	TP				FP				FN				TN			
	FS	PI	PCA	aiMRS	FS	PI	PCA	aiMRS	FS	PI	PCA	aiMRS	FS	PI	PCA	aiMRS
PNN	74	79	78	81	2	1	1	0	11	6	7	4	54	55	55	56
ELM	76	79	79	83	2	1	1	0	9	6	6	2	54	55	55	56
SVM	75	78	79	83	2	1	1	1	10	7	6	2	54	55	55	55
LDA	74	77	78	80	3	2	3	1	11	8	8	5	55	54	53	55
k-NN	70	73	72	78	4	3	3	2	15	12	13	7	52	53	53	54
Bayes	67	70	70	75	8	6	7	3	18	15	15	10	48	50	49	53

Table 7 Performance comparisons of obtained classification results for differentiation of benign and malignant brain tumours in the second experiment

Classifiers	Performance metrics																			
	ACC				SEN				SPE				PDV				NDV			
	FS	PI	PCA	aiMRS	FS	PI	PCA	aiMRS	FS	PI	PCA	aiMRS	FS	PI	PCA	aiMRS	FS	PI	PCA	aiMRS
PNN	91.49	95.04	94.33	97.16	87.06	92.94	91.76	95.29	96.43	98.21	98.21	100	97.37	98.75	98.73	100	83.08	90.16	88.71	93.33
ELM	92.20	95.04	95.04	98.58	89.41	92.94	92.94	97.65	96.43	98.21	98.21	100	97.44	98.75	98.75	100	87.31	90.16	90.16	96.55
SVM	91.49	94.33	95.04	97.87	88.24	91.76	92.94	97.65	96.43	98.21	98.21	98.21	97.40	98.73	98.75	98.81	84.38	88.71	90.16	96.49
LDA	91.49	90.97	92.91	95.75	87.06	90.59	91.76	94.11	98.21	96.43	94.64	98.21	96.10	97.47	96.30	98.77	83.33	87.10	86.89	91.67
k-NN	86.52	89.36	88.65	93.62	82.35	85.88	84.71	91.76	92.86	94.64	94.64	96.43	94.60	96.05	96.0	97.50	77.61	81.54	80.31	88.52
Bayes	81.56	85.11	84.40	90.78	78.82	82.35	82.35	88.24	85.71	89.29	87.50	94.64	89.33	92.11	90.91	96.15	72.73	76.92	76.56	84.13

Fig. 13, there are some differences between the MRS signal of a patient with benign MEN brain tumour used for training and the MRS signal of a patient with GBM brain tumour used for testing. The most significant of these differences is that there is an excessive increase in Lac + Lip peaks in the frequency range of 1.3 ppm to 1.4 ppm in the GBM test signal and an excessive decrease in NAA peak in the frequency value of approximately 2.02 ppm.

The confusion matrix showing the results obtained from the detailed experiments performed for the differentiation of benign and malignant brain tumour cases is presented in Table 6 and the analysis of the performance criteria are presented in Table 7. When the performance results for the differentiation of MEN and GBM brain tumours are examined, it is obtained that when the feature is extracted by aiMRS method and classification process is performed, successful results are obtained by ELM classifier as 98.58% ACC. In addition, if aiMRS is selected as feature extraction method in second experiment, more successful results are obtained by ELM for other performance metrics such as SEN, SPE, PDV and NDV.

Primary brain tumours can affect the surrounding areas, while MET brain tumours can spread to the brain through blood. Whether a tumour occurs in the brain or it is a tumour metastasised from another organ is very important for the treatment method and planning. Therefore, in the third experiment, a test conducted on MRS signals to differentiate between primary brain tumours and MET brain tumours. In the experiment, MRS signals of MEN brain tumour for 56 cases and MET brain tumours for 39 cases were used to differentiate primary brain tumours and MET brain tumours.

In this experiment, the MRS signal of the MET brain tumour was first determined as a training set using NSA algorithm. The signals to be determined later were used as the test signal with the

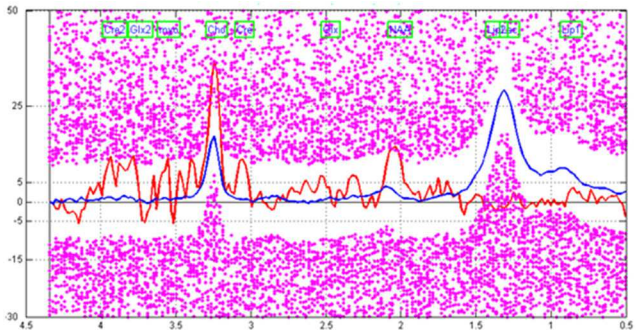

Fig. 14 *MRS training and test signals for MEN and MET brain tumours*

Table 8 Obtained confusion matrix using feature extraction and classification methods for the differentiation of primary and MET brain tumours in the third experiment

Classifier	TP				FP				FN				TN			
	FS	PI	PCA	aiMRS	FS	PI	PCA	aiMRS	FS	PI	PCA	aiMRS	FS	PI	PCA	aiMRS
PNN	32	37	36	38	4	2	3	0	7	2	3	1	52	54	53	56
ELM	33	37	37	38	4	1	2	0	6	2	2	1	52	55	52	56
SVM	30	36	37	38	3	1	3	1	9	3	2	1	53	55	53	55
LDA	30	35	35	38	3	3	4	1	9	4	4	1	53	53	52	55
k-NN	29	34	34	37	5	3	5	2	10	5	5	2	51	53	51	54
Bayes	27	32	30	34	9	5	7	5	12	7	9	5	46	51	48	51

Table 9 Performance comparisons of obtained classification results for differentiation of primary and MET brain tumours in the third experiment

Classifiers	Performance metrics																			
	ACC				SEN				SPE				PDV				NDV			
	FS	PI	PCA	aiMRS	FS	PI	PCA	aiMRS	FS	PI	PCA	aiMRS	FS	PI	PCA	aiMRS	FS	PI	PCA	aiMRS
PNN	88.42	95.79	92.94	98.94	82.05	94.87	92.31	97.44	92.86	96.43	94.64	100	88.89	94.87	92.31	100	88.14	96.43	94.64	98.25
ELM	89.47	96.84	93.68	98.94	84.62	94.87	94.87	97.44	92.86	98.21	98.21	100	89.19	97.37	94.87	100	89.66	96.49	96.30	98.25
SVM	87.37	92.63	94.74	97.89	76.92	92.31	94.87	97.44	94.64	98.21	94.64	98.21	90.91	97.30	92.50	97.44	85.48	94.83	96.37	98.21
LDA	87.37	92.63	91.58	97.89	76.92	89.74	89.74	97.44	94.64	94.64	92.88	98.21	90.91	92.11	89.74	97.44	85.48	92.98	92.88	96.43
k-NN	84.21	91.58	89.47	95.79	74.36	87.18	87.18	94.87	91.07	94.64	91.07	96.43	85.29	91.89	87.18	84.87	83.61	91.38	91.07	96.43
Bayes	76.84	87.37	82.11	89.47	69.23	82.05	76.92	87.18	82.14	91.07	85.71	91.07	75.0	86.49	81.08	87.18	79.31	87.93	84.21	91.07

optimal detector set. After detecting abnormal changes in the signal, the feature extraction for the classification of the signal was performed by aiMRS method proposed in this study. In Fig. 14, the MRS signal shown in blue colour indicates a training signal of a MET brain tumour and the red coloured MRS signal denoted test signal.

In addition, the optimum detector set of the test MRS signals of the patient with MEN brain tumour are shown as pink colour points. As seen in Fig. 14, there are some differences between the MRS signal of a patient with MET brain tumour used for training and the MRS signal of a patient with MEN brain tumour used for testing. An excessive increase was observed in Lac + Lip peaks at 1.3–1.4 ppm frequency ranges in MRS signal of MET brain tumour an excessive decrease was observed in NAA peak at 2.02 ppm frequency. In MEN brain tumours, there are excessive increases in average number of the activated detectors and average error rates compared to MET tumours. On the other hand, there are significant changes in the rates of some metabolites that could provide significant information about the tumour. A decrease in NAA/Cr, a decrease in Cho/Cr, a decrease in Cho/NAA, and a very extreme decrease in Lac/Cr can be deduced from this figure.

The results obtained from the detailed experiments performed for the differentiation of primary brain tumours and MET brain tumour cases are shown in Table 8. In addition, the performance analysis for this experiment is presented in Table 9. When the above test results obtained for the differentiation of MET and primary brain tumours are examined, it is seen that high accuracy results are obtained when the feature is extracted by aiMRS method and classification is performed ELM and PNN as 98.94% ACC. In addition, when PNN and ELM classification method is used, it is seen that the cases are differentiated more successfully for this experiment.

Some studies have been proposed for classification of brain tumours using MRS signal data. However, it is very difficult to compare all of these studies in terms of performance because most of these studies have different data sets and various methodologies. Nevertheless, as in Table 10, a comprehensive comparison of some studies for classification of brain tumours using MRS signals on INTERPRET database is summarised. This summary table shows that the method proposed in this study is successful in grading brain tumours when compared to other studies in terms of classification of normal versus tumour, low-grade versus high-grade and primary versus MET. In comparison for normal versus tumour, the results of this study have reached 100% ACC similar to Arizmendi *et al.* [58] and Arizmendi *et al.* [7]. In terms of comparison of low-grade versus high-grade, although the results in this study were obtained as 98.58% ACC, the results of Luts *et al.* [11] and Arizmendi *et al.* [7] were higher than the results of this study. Finally, for primary versus MET, the results of this study were obtained as 98.94% ACC and were higher than the others.

6 Conclusion

In this study, a hybrid feature extraction method called as aiMRS using MRS data is proposed for the diagnosis and classification of brain tumours. In the experimental studies, the distinction of benign and malignant brain tumours, differentiation of normal brain tissue and brain tumour and classification of MET brain tumours and primary brain tumours were performed with high accuracy using pattern recognition methods such as PNN, ELM,

Table 10 Comparison of the proposed method with other reported studies for classification of brain tumours on MRS data

The study	Data set	Data type	Feature extraction/ reduction method	Classification method	ACC		
					Normal versus tumour	Low-grade versus high-grade	Primary versus MET
Arizmendi *et al.* [58]	INTERPRET	MRS	moving window with variance analysis (MWVA), PCA	Bayesian neural networks	100	97.0	98.0
García-Gómez *et al.* [13]	INTERPRET and eTUMOUR	MRS	PI, PCA, ICA, wavelet, peak height of typical resonances and FS	LDA, FLDA, multi-layer perceptron and LS-SVM	90.0	91.0	97.0
Tate *et al.* [30]	INTERPRET	MRS	correlation coefficients using a DSS	LDA	NA	*89.0*	*NA*
Arizmendi *et al.* [7]	INTERPRET	MRS	Gaussian decomposition, MWVA	Bayesian neural networks	100	98.75	*95.0*
Luts *et al.* [11]	INTERPRET	MRI and MRSI	Kruskal–Wallis test, relief-F, fisher discriminant	LS-SVM, LDA	99.84	100	*NA*
proposed study	INTERPRET	MRS	aiMRS	ELM, PNN, SVM, Bayes, LDA and *k*-NN	100	98.58	98.94

NA: not applicable

Bayes, *k*-NN, LDA and SVM. When the feature extraction is performed using aiMRS, the differentiation of normal brain tissue and brain tumours, the distinction of benign and malignant tumours and MET with primary brain tumours were achieved with 100, 98.58 and 98.94% ACC, respectively. As a result, the proposed method can be used as a secondary tool for the detection of brain tumours on MRS data.

The contributions of this proposed method are as follows. Classification of brain tumours on MRS can be achieved with a proposed method with high accuracy. When the studies in the literature are examined, it is seen that classification procedures of brain tumours are handled separately. On the other hand, the proposed method enables performing all procedures with high performance. In addition, the results of some previous studies as seen in Table 10 were improved using the proposed method on INTERPRET database. Besides being robust, the developed method can perform extremely fast as it does not require heavy computation load. In the test stage, a detection process on a standard computer could be completed by ELM in ~2 s using the proposed method. The proposed method is advantageous in terms of usability in the clinical setting as compared to complex methods requiring heavy processing load. Performance evaluations of the proposed method are carried out in detail with a large database (INTERPRET) obtained from different devices. The fact that the MRS signals in the database are obtained from different imaging devices enabled the proposed method to undergo a detailed test process in accordance with the clinical conditions.

Non-invasive methods such as MRS are important for detection of brain tumours where MRI is inadequate in most cases. However, MRS is still not routinely used in clinical setting. The reason of this is the need to develop various methods for collecting data from MRS devices, analysing the spectrum and presenting the data in a simple and visual way. In addition, the availability of MRS should be demonstrated through multicenter and evidence-based research. MRS signals obtained from brain tumours contain chemical information about the characteristics of metabolites for tumour types. However, a good classifier designed to classify different brain tumours using MRS signals also contains problems due to several factors. For example, when short TE ^{1}H-MRS spectrum data are used, it can be seen that the GBM signal patterns are classified as MET or primary brain tumours. This is because MET and GBM brain tumours are very similar to MRS signal patterns. In order to eliminate these problems, training and testing procedures can be carried out with classification methods on more signal patterns. In addition, the presence of noise and measurement errors in the spectrum signal may also cause signal distortion. As a result, it becomes difficult to obtain the same pattern continuously in the signal. In this study, MRS scans were performed according to single-voxel and short TE for classification of brain tumours. In next works, the performance of multi-voxel and long TE in tumour detection can be evaluated. In addition, the MRS signals were acquired with a 1.5 T scanner. For the following studies, the evaluation of MRS signals from 3 or 7 T scanners can be an important study. Moreover, the success of new generation 3D MRS scanners on the classification of tumours can be investigated.

7 Acknowledgments

The author thanks all the stakeholders of the project, especially Dr Maria Margarida Julià-Sapé, for allowing the use of MRS data in the INTERPRET database.

8 References

[1] 'ASCO's state of cancer care in America', Available at https://www.asco.org/research-progress/reports-studies/state-cancer-care, accessed 27 October 2019

[2] 'Cancer facts & figures 2019', Available at https://www.cancer.org/content/dam/cancer-org/research/cancer-facts-and-statistics/annual-cancer-facts-and-figures/2019/cancer-facts-and-figures-2019.pdf, accessed 10 October 2019

[3] 'Cancer today: data visualization tools for exploring the global cancer burden in 2018', Available at http://gco.iarc.fr/today/home, accessed 28 July 2019

[4] Bray, F., Ferlay, J., Soerjomataram, I., *et al.*: 'Global cancer statistics 2018: globocan estimates of incidence and mortality worldwide for 36 cancers in 185 countries', *CA-Cancer J. Clin.*, 2018, **68**, (6), pp. 394–424

[5] Ari, A., Hanbay, D.: 'Tumor detection in Mr images of regional convolutional neural networks', *J. Fac. Eng. Archit. Gazi Univ.*, 2019, **34**, (3), pp. 1395–1408

[6] Howe, F.A., Opstad, K.S.: '1 h MR spectroscopy of brain tumours and masses', *NMR Biomed.*, 2003, **16**, (3), pp. 123–131

[7] Arizmendi, C., Sierra, D.A., Vellido, A., *et al.*: 'Automated classification of brain tumours from short Echo time in vivo MRS data using Gaussian decomposition and Bayesian neural networks', *Expert Syst. Appl.*, 2014, **41**, (11), pp. 5296–5307

[8] Postma, G.J., Luts, J., Idema, A.J., *et al.*: 'On the relevance of automatically selected single-voxel MRS and multimodal MRI and MRSI features for brain tumour differentiation', *Comput. Biol. Med.*, 2011, **41**, (2), pp. 87–97

[9] Sáez, C., Martí-Bonmatí, L., Alberich-Bayarri, Á., *et al.*: 'Randomized pilot study and qualitative evaluation of a clinical decision support system for brain tumour diagnosis based on Sv 1 h MRS: evaluation as an additional information procedure for novice radiologists', *Comput. Biol. Med.*, 2014, **45**, pp. 26–33

[10] Vicente, J., Fuster-Garcia, E., Tortajada, S., *et al.*: 'Accurate classification of childhood brain tumours by in Vivo1 HMRS–a multi-centre study', *Eur. J. Cancer*, 2013, **49**, (3), pp. 658–667

[11] Luts, J., Heerschap, A., Suykens, J.A., *et al.*: 'A combined MRI and MRS based multiclass system for brain tumour recognition using LS-SVMS with class probabilities and feature selection', *Artif. Intell. Med.*, 2007, **40**, (2), pp. 87–102

[12] Wang, Q., Liacouras, E.K., Miranda, E., *et al.*: 'Classification of brain tumors using MRI and MRS data'. Medical Imaging 2007: Computer-Aided Diagnosis, San Diego, CA, USA., 2007, p. 65140S

[13] García-Gómez, J.M., Luts, J., Julià-Sapé, M., *et al.*: 'Multiproject–multicenter evaluation of automatic brain tumor classification by magnetic resonance spectroscopy', *Magn. Reson. Mater. Phys. Biol. Med.*, 2009, **22**, (1), p. 5

[14] Georgiadis, P., Kostopoulos, S., Cavouras, D., *et al.*: 'Quantitative combination of volumetric Mr imaging and Mr spectroscopy data for the

discrimination of meningiomas from metastatic brain tumors by means of pattern recognition', *Magn. Reson. Imaging*, 2011, **29**, (4), pp. 525–535
[15] Ross, B., Michaelis, T.: 'Clinical applications of magnetic resonance spectroscopy', *Magn. Reson. Q.*, 1994, **10**, (4), pp. 191–247
[16] Bulik, M., Jancalek, R., Vanicek, J., *et al.*: 'Potential of MR spectroscopy for assessment of glioma grading', *Clin. Neurol. Neurosurg.*, 2013, **115**, (2), pp. 146–153
[17] Bruhn, H., Frahm, J., Gyngell, M.L., *et al.*: 'Noninvasive differentiation of tumors with use of localized H-1 MR spectroscopy in vivo: initial experience in patients with cerebral tumors', *Radiology*, 1989, **172**, (2), pp. 541–548
[18] Castillo, M., Kwock, L., Scatliff, J., *et al.*: 'Proton MR spectroscopy in neoplastic and non-neoplastic brain disorders', *Magn. Reson. Imaging Clin. N Am.*, 1998, **6**, (1), pp. 1–20
[19] Howe, F., Barton, S., Cudlip, S., *et al.*: 'Metabolic profiles of human brain tumors using quantitative in vivo 1 h magnetic resonance spectroscopy', *Magn. Reson. Med.*, 2003, **49**, (2), pp. 223–232
[20] Klose, U.: 'In vivo proton spectroscopy in presence of eddy currents', *Magn. Reson. Med.*, 1990, **14**, (1), pp. 26–30
[21] López-Villegas, D., Lenkinski, R.E., Wehrli, S.L., *et al.*: 'Lactate production by human monocytes/macrophages determined by proton MR spectroscopy', *Magn. Reson. Med.*, 1995, **34**, (1), pp. 32–38
[22] Pouwels, P.J., Frahm, J.: 'Regional metabolite concentrations in human brain as determined by quantitative localized proton MRS', *Magn. Reson. Med.*, 1998, **39**, (1), pp. 53–60
[23] Castillo, M., Smith, J.K., Kwock, L.: 'Correlation of myo-inositol levels and grading of cerebral astrocytomas', *Am. J. Neuroradiol.*, 2000, **21**, (9), pp. 1645–1649
[24] Porto, L., Kieslich, M., Franz, K., *et al.*: 'Mr spectroscopy differentiation between high and low grade astrocytomas: A comparison between paediatric and adult tumours', *Eur. J. Paediatr. Neurol.*, 2011, **15**, (3), pp. 214–221
[25] Server, A., Kulle, B., Gadmar, Ø.B., *et al.*: 'Measurements of diagnostic examination performance using quantitative apparent diffusion coefficient and proton MR spectroscopic imaging in the preoperative evaluation of tumor grade in cerebral gliomas', *Eur. J. Radiol.*, 2011, **80**, (2), pp. 462–470
[26] Majos, C., Aguilera, C., Alonso, J., *et al.*: 'Proton MR spectroscopy improves discrimination between tumor and pseudotumoral lesion in solid brain masses', *Am. J. Neuroradiol.*, 2009, **30**, (3), pp. 544–551
[27] Tsolaki, E., Svolos, P., Kousi, E., *et al.*: 'Automated differentiation of glioblastomas from intracranial metastases using 3t Mr spectroscopic and perfusion data', *Int. J. Comput. Assist. Radiol. Surg.*, 2013, **8**, (5), pp. 751–761
[28] Preul, M.C., Caramanos, Z., Collins, D.L., *et al.*: 'Accurate, noninvasive diagnosis of human brain tumors by using proton magnetic resonance spectroscopy', *Nat. Med.*, 1996, **2**, (3), p. 323
[29] De Edelenyi, F.S., Rubin, C., Esteve, F., *et al.*: 'A new approach for analysing proton magnetic resonance spectroscopic images of brain tumors: nosologic images', *Nat. Med.*, 2000, **6**, (11), p. 1287
[30] Tate, A.R., Underwood, J., Acosta, D.M., *et al.*: 'Development of a decision support system for diagnosis and grading of brain tumours using in vivo magnetic resonance single voxel Spectra', *NMR Biomed.*, 2006, **19**, (4), pp. 411–434
[31] Lukas, L., Devos, A., Suykens, J.A., *et al.*: 'Brain tumor classification based on long Echo proton MRS signals', *Artif. Intell. Med.*, 2004, **31**, (1), pp. 73–89
[32] 'International network for pattern recognition of tumours using magnetic resonance', Available at http://gabrmn.uab.es/interpret/, accessed: 27/10/2019
[33] 'Etumour database portal', Available at http://solaria.uab.es/eTumour/, accessed 27 October 2019
[34] Majós, C., Julià-Sapé, M., Alonso, J., *et al.*: 'Brain tumor classification by proton MR spectroscopy: comparison of diagnostic accuracy at short and long Te', *Am. J. Neuroradiol.*, 2004, **25**, (10), pp. 1696–1704
[35] Devos, A., Simonetti, A., Van Der Graaf, M., *et al.*: 'The use of multivariate Mr imaging intensities versus metabolic data from Mr spectroscopic imaging for brain tumour classification', *J. Magn. Reson.*, 2005, **173**, (2), pp. 218–228
[36] Nachimuthu, D.S., Baladhandapani, A.: 'Multidimensional texture characterization: on Analysis for brain tumor tissues using MRS and MRI', *J. Digit. Imaging*, 2014, **27**, (4), pp. 496–506
[37] Wang, L., Wan, S., Sun, Y., *et al.*: 'Automatic classification of brain tumor by in vivo MRS data based on LDA and SVM'. Seventh Int. Conf. on Measuring Technology and Mechatronics Automation, Nanchang, China, 2015, pp. 213–216
[38] Hajek, M., Dezortova, M.: 'Introduction to clinical in vivo Mr spectroscopy', *Eur. J. Radiol.*, 2008, **67**, (2), pp. 185–193
[39] Callot, V., Galanaud, D., Le Fur, Y., *et al.*: '1 h MR spectroscopy of human brain tumours: A practical approach', *Clin. Imaging*, 2008, **67**, (2), pp. 268–274
[40] Soares, D., Law, M.: 'Magnetic resonance spectroscopy of the brain: review of metabolites and clinical applications', *Clin. Radiol.*, 2009, **64**, (1), pp. 12–21
[41] Julià-Sapé, M., Acosta, D., Mier, M., *et al.*: 'A multi-centre, web-accessible and quality control-checked database of in vivo Mr Spectra of brain tumour patients', *Magn. Reson. Mater. Phys. Biol. Med.*, 2006, **19**, (1), pp. 22–33
[42] García-Gómez, J.M., Tortajada, S., Vidal, C., *et al.*: 'The effect of combining two Echo times in automatic brain tumor classification by mrs', *NMR Biomed.*, 2008, **21**, (10), pp. 1112–1125
[43] Timmis, J., Knight, T., de Castro, L.N., *et al.*: 'An overview of artificial immune systems', in '*Computation in cells and tissues*' (Springer, Germany, 2004), pp. 51–91
[44] Çalış, H., Çakır, A., Dandil, E.: 'Artificial immunity-based induction motor bearing fault diagnosis', *Turkish J. Electr. Eng. Comput. Sci.*, 2013, **21**, (1), pp. 1–25
[45] Forrest, S., Perelson, A.S., Allen, L., *et al.*: 'Self-nonself discrimination in a computer'. Proc. 1994 IEEE Computer Society Symp. on Research in Security and Privacy, Oakland, CA, USA., 1994, pp. 202–212
[46] De Castro, L.N., Timmis, J.: '*Artificial immune systems: A new computational intelligence approach*' (Springer Science & Business Media, Germany, 2002)
[47] Gonzalez, F., Dasgupta, D., Kozma, R.: 'Combining negative selection and classification techniques for anomaly detection'. Proc. 2002 Congress on Evolutionary Computation. CEC'02 (Cat. No. 02TH8600), Honolulu, HI, USA., 2002, pp. 705–710
[48] De Castro, L.N., Von Zuben, F.J.: 'Learning and optimization using the clonal selection principle', *IEEE Trans. Evol. Comput.*, 2002, **6**, (3), pp. 239–251
[49] Ada, G.L., Nossal, S.G.: 'The clonal-selection theory', *Sci. Am.*, 1987, **257**, (2), pp. 62–69
[50] Gao, X.Z., Ovaska, S.J., Wang, X., *et al.*: 'Clonal optimization-based negative selection algorithm with applications in motor fault detection', *Neural Comput. Appl.*, 2009, **18**, (7), pp. 719–729
[51] Tognarelli, J.M., Dawood, M., Shariff, M.I., *et al.*: 'Magnetic resonance spectroscopy: principles and techniques: lessons for clinicians', *J. Clin. Exp. Hepatol.*, 2015, **5**, (4), pp. 320–328
[52] Stern, A.S., Donoho, D.L., Hoch, J.C.: 'NMR data processing using iterative thresholding and Minimum L1-norm reconstruction', *J. Magn. Reson.*, 2007, **188**, (2), pp. 295–300
[53] Devos, A., Lukas, L., Suykens, J., *et al.*: 'Classification of brain tumours using short Echo time 1 h MR Spectra', *J. Magn. Reson.*, 2004, **170**, (1), pp. 164–175
[54] Govindaraju, V., Young, K., Maudsley, A.A.: 'Proton NMR chemical shifts and coupling constants for brain metabolites', *NMR Biomed.*, 2000, **13**, (3), pp. 129–153
[55] Burges, C.J.: 'Geometric methods for feature extraction and dimensional reduction-a guided tour', in '*Data mining and knowledge discovery handbook*', (Springer, USA, 2009), pp. 53–82
[56] Fukunaga, K.: '*Introduction to statistical pattern recognition*' (Elsevier, USA., 2013)
[57] Ma, J., Sun, Z.: 'Mrs classification based on independent component analysis and support vector machines'. Fifth Int. Conf. on Hybrid Intelligent Systems (HIS'05), Rio de Janeiro, Brazil, 2005, p. 3
[58] Arizmendi, C., Vellido, A., Romero, E.: 'Classification of human brain tumours from MRS data using discrete wavelet transform and Bayesian neural networks', *Expert Syst. Appl.*, 2012, **39**, (5), pp. 5223–5232
[59] Opstad, K., Ladroue, C., Bell, B., *et al.*: 'Linear discriminant analysis of brain tumour 1 h Mr Spectra: A comparison of classification using whole Spectra versus metabolite quantification', *NMR Biomed.*, 2007, **20**, (8), pp. 763–770
[60] Luts, J., Vandermeulen, D., Heerschap, A., *et al.*: 'Classification of brain tumors based on magnetic resonance spectroscopy'. PhD thesis, Faculty of Engineering, KU Leuven, Leuven, Belgium, 2010
[61] Specht, D.F.: 'Probabilistic neural networks', *Neural Netw.*, 1990, **3**, (1), pp. 109–118
[62] Mao, K.Z., Tan, K.-C., Ser, W.: 'Probabilistic neural-network structure determination for pattern classification', *IEEE Trans. Neural Netw.*, 2000, **11**, (4), pp. 1009–1016
[63] Kumar, S., Moni, R., Rajeesh, J.: 'An automatic computer-aided diagnosis system for liver tumours on computed tomography images', *Comput. Electr. Eng.*, 2013, **39**, (5), pp. 1516–1526
[64] Huang, G.-B., Zhu, Q.-Y., Siew, C.-K.: 'Extreme learning machine: A new learning scheme of feedforward neural networks'. 2004 IEEE int. joint Conf. on neural networks (IEEE Cat. No. 04CH37541), Budapest, Hungary, 2004, pp. 985–990
[65] Pradhan, M.K., Minz, S., Shrivastava, V.K.: 'Fast active learning for hyperspectral image classification using extreme learning machine', *IET Image Process.*, 2018, **13**, (4), pp. 549–555
[66] Zhang, W., Ji, H.: 'Fuzzy extreme learning machine for classification', *IET Electron. Lett.*, 2013, **49**, (7), pp. 448–450
[67] Agrawal, R., Bala, R.: 'Incremental Bayesian classification for multivariate normal distribution data', *Pattern Recognit. Lett.*, 2008, **29**, (13), pp. 1873–1876
[68] Vapnik, V.: '*The nature of statistical learning theory*' (Springer Science & Business Media, USA., 2013)
[69] Yücesoy, E., Nabiyev, V.: 'Determination of a speaker's age and gender with an SVM classifier based on GMM supervectors', *J. Fac. Eng. Archit. Gazi Univ.*, 2016, **31**, (3), pp. 501–509
[70] Küçük, H., Eminoğlu, İ., Balci, K.: 'Classification of neuromuscular diseases with artificial intelligence methods', *J. Fac. Eng. Archit. Gazi Univ.*, 2019, **34**, (4), pp. 1725–1742
[71] Khan, T., Westin, J., Dougherty, M.: 'Classification of speech intelligibility in Parkinson's disease', *Biocybern. Biomed. Eng.*, 2014, **34**, (1), pp. 35–45
[72] Shen, J., Pei, Z., Fisher, G., *et al.*: 'Modelling and analysis of waviness reduction in soft-pad grinding of wire-sawn silicon wafers by support vector regression', *Int. J. Prod. Res.*, 2006, **44**, (13), pp. 2605–2623
[73] Zheng, W., Zhao, L., Zou, C.: 'Locally nearest neighbor classifiers for pattern classification', *Pattern Recognit.*, 2004, **37**, (6), pp. 1307–1309
[74] Mitchell, H., Schaefer, P.: 'A 'soft' K-nearest neighbor voting scheme', *Int. J. Intell. Syst.*, 2001, **16**, (4), pp. 459–468
[75] Duda, R.O., Hart, P.E., Stork, D.G.: '*Pattern classification*' (John Wiley & Sons, USA., 2012)
[76] Ripley, B.D.: '*Pattern recognition and neural networks*' (Cambridge University Press, USA., 2007)
[77] 'Grup d'aplicacions biomèdiques De La ressonància magnètica nuclear (gabrmn) interpret dss', Available at http://gabrmn.uab.es/dss, accessed: 27/10/2019